

# Light scattering in superionic glasses $(\text{AgI})_x(\text{AgPO}_3)_{1-x}$ : Brillouin and Raman scattering

P. Benassi, A. Fontana, and P. A. M. Rodrigues\*

*Dipartimento di Fisica, Università degli Studi di Trento  
e Unità di Trento del Consorzio Interuniversitario di Fisica della Materia,  
I-38050 Povo (Trento), Italy*

(Received 6 June 1990)

Brillouin and Raman-scattering experiments have been performed on the fast-ion conductor  $(\text{AgI})_x(\text{AgPO}_3)_{1-x}$  in the full glass-forming region ( $0 < x < 0.55$ ) from 18 to 330 K. We have been able to cover the full spectral range ( $0.2 < \omega < 350 \text{ cm}^{-1}$ ) in this kind of solid-state sample by using the same spectrometer. The Raman spectra generally show a quasielastic scattering and two bumps centered at 30 and  $110 \text{ cm}^{-1}$ , with the last one being present only in the polarized configuration. By increasing the AgI content, the behavior of the Brillouin and Raman intensities together with the Raman spectral shape suggests the hypothesis that the Raman scattering of such glasses can be reconstructed by the sum of the pure  $\alpha$ -AgI and  $\text{AgPO}_3$  spectra. Hence in these glasses the vibrational dynamics of pure  $\alpha$ -AgI and  $\text{AgPO}_3$  seems to be weakly interacting with each other. Our data are compatible with the hypothesis that the structure of these glasses is formed by clusters of AgI dispersed in the  $\text{AgPO}_3$  host matrix.

## I. INTRODUCTION

The superionic glass family  $(\text{AgI})_x(\text{AgPO}_3)_{1-x}$  exhibits interesting dynamical properties together with fast-ion diffusion of the cations.<sup>1</sup> The pure  $\text{AgPO}_3$  is a glass with poor conductivity while the AgI is one of the superionic conductors with higher conductivity. Indeed the latter is a widely studied system: at  $147^\circ\text{C}$  it goes through a first-order phase transition from an ordered wurtzitelike structure ( $\beta$  phase) to a cubic one ( $\alpha$  phase). After the phase transition the ionic conductivity increases by more than four orders of magnitude.<sup>2</sup> A possible explanation of the high ionic conductivity<sup>2</sup> is that this last phase is not a completely ordered one because the  $\text{Ag}^+$  ions have several equivalent and semiequivalent structural sites favoring the  $\text{Ag}^+$  travel.

The easy procedure in varying the AgI concentration in the glasses  $(\text{AgI})_x(\text{AgPO}_3)_{1-x}$  allows us to study the dynamical and structural changes of the system for a wide range of silver iodide content.

The main problem in the study of the AgI-based glasses is understanding the role of silver iodide in connection with the ionic conductivity. By means of neutron diffraction<sup>3</sup> and inelastic neutron scattering,<sup>4,5</sup> the possibility has been shown of the existence of small clusters of distorted tetrahedra of silver iodide dispersed in the host matrix.

In some previous works<sup>6-9</sup> about silver-iodide-silver-borate glasses, one of us (A.F.) interpreted the Raman scattering as being mainly due to AgI, which is expected to strongly contribute to the polarizability of the system. In those papers it has been hypothesized that AgI tends to reproduce connected and distorted tetrahedra and such a connection would favor the  $\text{Ag}^+$  conductivity,

thus allowing the travel through some diffusion paths due to the presence of many sites in the AgI units.

In this work we present light-scattering results obtained by coupling two different scattering techniques (i.e., the Raman and the Brillouin techniques) in the study of silver-phosphate glasses in a wide range of temperatures (from 18 to 330 K) and AgI content ( $0 < x < 0.55$ ). The goal of these measurements, with respect to those previously reported in literature, has been the possibility of covering, in this kind of solid state sample, the full spectral range ( $0.2\text{--}350 \text{ cm}^{-1}$ ) by using the same spectrometer.<sup>10</sup>

In this first paper we will focus our attention on a quantitative description of the spectrum in the frequency range  $\omega < 350 \text{ cm}^{-1}$ . In a second paper we will discuss the origin of the low-frequency contribution to the Raman spectrum, also called quasielastic scattering (QES), which is presently a subject of great interest.

## II. EXPERIMENT

### A. Sample preparation and characterization

Disk-shaped samples (30 mm diam, 2 mm thickness) were prepared in our laboratory following a standard procedure<sup>1</sup> employing appropriate amounts of AgI and  $\text{H}_3\text{PO}_4$ . In order to have a complete reduction, the powders were heated at first in a quartz crucible at 700 K for 2 h, then the melted solution was obtained by further heating at 800 K for 5 h. Quenching was obtained by rapidly pouring and pressing the melted compounds onto a steel mask kept at about 400 K. Finally the sample was annealed at  $T < T_g$  with the aim of minimizing the thermal stress. We have controlled the chemical com-

position and measured the glass temperature  $T_g$  and the mass density  $\rho$ , thus obtaining data in good agreement with those reported by other authors.<sup>1</sup> Beyond that, by x-ray-diffraction measurements we have verified that no crystalline microdomains were present in our samples.

We have prepared the  $\text{AgPO}_3$  glass and  $(\text{AgI})_x(\text{AgPO}_3)_{1-x}$  glasses at  $x = 0.1, 0.2, 0.3, 0.4, 0.5$ , and  $0.55$  concentrations, in order to explore the full glass-forming region. The samples were polished, thus obtaining good optical surfaces with roughness of the order of  $1 \mu\text{m}$ .

Crystalline pure  $\alpha\text{-AgI}$  were grown in an optical oven by Lars Borjesson using a procedure described elsewhere.<sup>11</sup>

### B. Experimental setup

Measurements were performed by a vertically polarized single mode  $\text{TM}_{00}$  Spectra Physics 2020 argon-ion laser operating with the  $5145\text{-}\text{\AA}$  line. The nominal laser power was kept under  $30 \text{ mW}$  in order to avoid sample heating and darkening, which is due to the photosensitivity of the glasses.<sup>6</sup>

The scattered light was analyzed by a SOPRA DPDM2000 monochromator after having selected the desired polarization. The monochromator operated in a single pass double monochromator configuration<sup>10</sup> at the 11th diffraction order. In this condition the limiting resolution was  $0.04 \text{ cm}^{-1}$  with a slit width of  $20 \mu\text{m}$ . A  $90^\circ$  scattering geometry was adopted, and polarized ( $VV$ ) and depolarized ( $HV$ ) spectra have been collected.

A four optical window flux cryostat was employed for sample cooling with a thermoregulation within  $1 \text{ K}$  from  $18 \text{ K}$  to room temperature.

The spectra were taken at several different resolutions in order to eliminate the stray light component. The connection of different resolution spectra allowed us to have reliable data from  $0.2$  to  $350 \text{ cm}^{-1}$ . After this connection our data were corrected for dark counts and for frequency- and polarization-dependent overall transmissivity.

Finally a nearly flat luminescence background has been parametrized and subtracted from our spectra.

## III. RESULTS

In this section we present the experimental results obtained following the procedure described in the previous section. In Fig. 1 the  $x = 0.4$  room-temperature spectrum in the polarized ( $VV$ ) and depolarized ( $HV$ ) configurations is shown in the frequency range between  $-1$  and  $250 \text{ cm}^{-1}$ , where the Brillouin doublet is seen together with the Raman scattering. The  $VV$  as well as the  $HV$  Raman spectra are roughly composed of a long-tail quasielastic contribution plus a broadband centered around  $20 \text{ cm}^{-1}$ . Only in the polarized spectrum is a second broad contribution around  $110 \text{ cm}^{-1}$  present. The behavior of the Raman spectral shape at several AgI con-

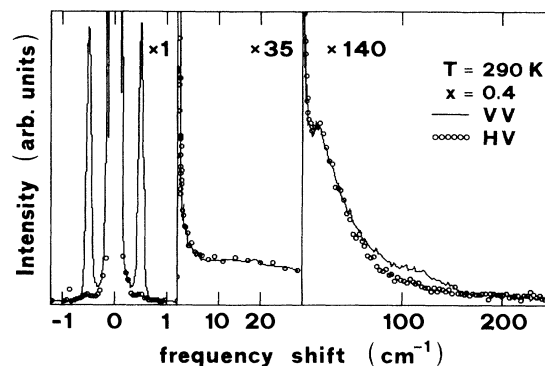


FIG. 1. Polarized (solid line) and depolarized (circles) spectra of the room-temperature  $x = 0.4$  glass. The two spectra are superimposed to emphasize the different spectral shape in the three considered frequency domains.

tents and temperatures is shown in Fig. 2. It should be noted that by increasing the AgI concentration [see Fig. 2(a)] the band centered at  $110 \text{ cm}^{-1}$  (which is absent at  $x = 0.0$ ) increases, together with a strong growth of the QES which at  $x = 0.55$  completely merges the band at  $20 \text{ cm}^{-1}$ . A similar behavior regarding the QES has been found increasing the temperature at a given AgI content, as Fig. 2(b) shows.

Finally let us consider the Brillouin scattering. In Fig. 3 we report the room-temperature Brillouin doublet obtained from  $(\text{AgI})_x(\text{AgPO}_3)_{1-x}$  glasses at two different concentrations of silver iodide and in pure  $(\text{AgPO}_3)$ . A Brillouin shift decrease can be seen at increasing  $x$ . Due to the high elastic scattering (caused by some imperfection present in our samples) and to our limited rejection, we have not obtained reliable data for the transverse Brillouin peaks, even if in some cases they were detected (see

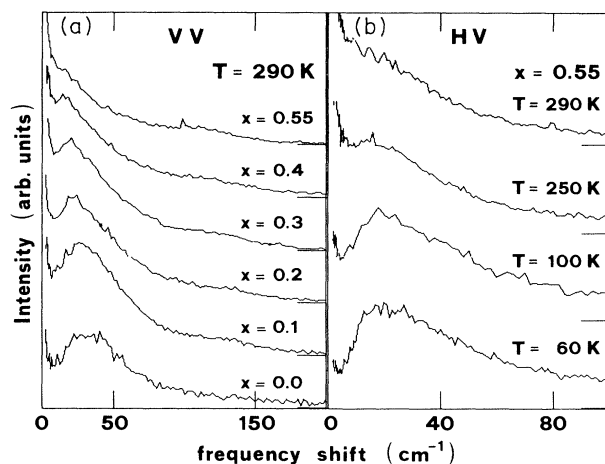


FIG. 2. Raman scattering from  $(\text{AgI})_x(\text{AgPO}_3)_{1-x}$  glasses. (a) Polarized room-temperature spectra obtained at different AgI concentrations from  $x = 0$  (i.e.,  $\text{AgPO}_3$ ) to  $x = 0.55$ . (b) Temperature behavior of the depolarized spectral shape for the  $x = 0.55$  glass from  $60$  to  $290 \text{ K}$ .

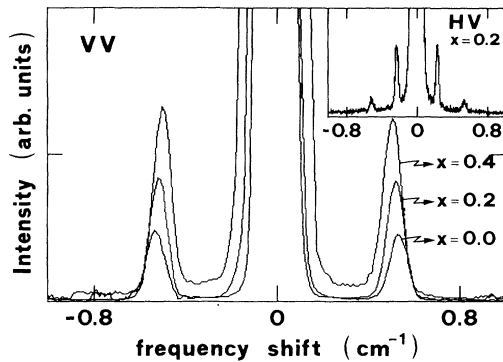


FIG. 3. Room-temperature longitudinal Brillouin doublet of  $(\text{AgI})_x(\text{AgPO}_3)_{1-x}$  glass family at three different AgI contents:  $x = 0.0, 0.2, 0.4$ . The inset shows the transverse modes collected in HV configuration at  $x = 0.2$ . The weak peaks at about  $0.5 \text{ cm}^{-1}$  are the spillover of the longitudinal peaks.

the inset of Fig. 3). The measured longitudinal Brillouin linewidth was found to be due to our experimental resolution so that no attempts have been made to extract information about the longitudinal kinematic viscosity coefficient from our spectra.

#### IV. DATA ANALYSIS AND DISCUSSION

To introduce our analysis, we divide the whole spectrum into three main frequency domains: (i) The very-low-frequency range  $0 < \omega < 1 \text{ cm}^{-1}$  (Brillouin doublet); (ii) The low-frequency range  $1 < \omega < 250 \text{ cm}^{-1}$  (QES and one-phonon density of states); (iii) The high-frequency range  $250 < \omega < 1300 \text{ cm}^{-1}$  (molecular structures domain).

The last one has been carefully analyzed in previous works.<sup>12,13</sup> The two main features in the Raman spectrum of the pure  $\text{AgPO}_3$  (centered around  $675$  and  $1142 \text{ cm}^{-1}$ ) are assigned to the stretching modes of the  $\text{PO}_4$  units. The addition of silver iodide does not affect the spectral shape in this frequency domain, while the peaks intensities (related to those of the pure  $\text{AgPO}_3$ ) decrease at increasing AgI content, this being due trivially to the diminishing quantity of  $\text{AgPO}_3$ . It may be argued, therefore, that the network formed by the  $\text{AgPO}_3$  matrix is not strongly modified by the insertion of silver iodide and this behavior is very similar in silver-borate glasses.<sup>6</sup>

As far as frequency domains (i) and (ii) are concerned, Fig. 1 shows that together with the low-frequency Brillouin doublet, also the high-frequency band centered around  $110 \text{ cm}^{-1}$  has a high degree of polarization.<sup>13</sup> Indeed, with the exception of these two spectral contributions, the shape of polarized and depolarized scattering is the same. This could suggest that  $VV$  and  $HV$  spectra can be treated in terms of isotropic and anisotropic contributions, but since we do not have the polarization ratio with the necessary accuracy, we will denote our spectra as isotropic and anisotropic just for a convenient way of discussing our data. Therefore, in the following we will

define

$$I_{\text{iso}}(\omega) = I_{VV}(\omega) - cI_{HV}(\omega), \quad (1)$$

$$I_{\text{aniso}}(\omega) = I_{HV}(\omega), \quad (2)$$

where  $c$  is the appropriate factor to normalize the  $VV$  and  $HV$  spectra in the range where they have the same spectral shape (see Fig. 1).

#### A. Isotropic scattering

As is shown in Fig. 4, two main features contribute to the isotropic spectrum: the low-frequency Brillouin doublet and the high-frequency structure centered around  $110 \text{ cm}^{-1}$ .

##### 1. Brillouin shifts and sound velocities

The longitudinal Brillouin shifts as measured from our spectra are reported in Fig. 5, at all AgI concentrations and temperatures.

Beyond the fact that for all AgI contents the glasses become less rigid at high temperatures, Fig. 5 shows that for  $x = 0.55$  the elastic constant changes in a linear way in this temperature range, and a similar behavior can also be inferred for all our samples. Our values are generally slightly higher (5%) than those extrapolated from the data reported in the literature<sup>14</sup> and this could be due to a small difference in the refractive index at the wavelength used by us and the one in Ref. 14.

Using our mass density and Brillouin-shift measurements and the refractive index values from Ref. 14 we have obtained the longitudinal sound velocities (see Table I). Again, at increasing AgI concentration, the glass structure becomes less rigid and therefore we observe a decreasing sound velocity that tends linearly to that of the  $\alpha$ -AgI (see Fig. 6).

##### 2. Brillouin intensities

The main goal of this work has been the possibility of evaluating the scattering intensities using the Brillouin

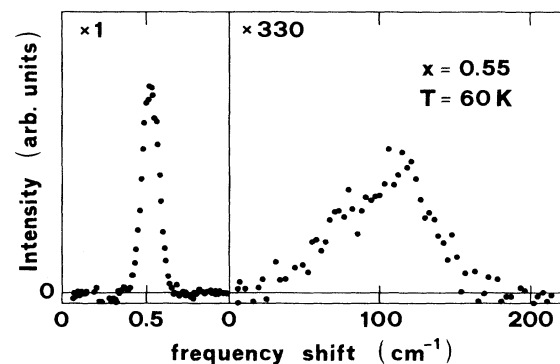


FIG. 4. Isotropic spectrum [see Eq. (1)] of  $(\text{AgI})_x(\text{AgPO}_3)_{1-x}$  at  $x = 0.55$  and  $T = 60 \text{ K}$ .

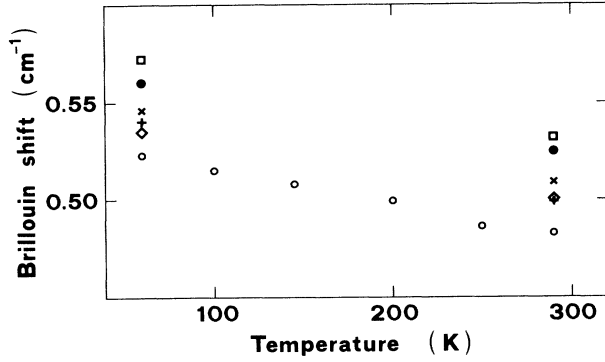


FIG. 5. Temperature behavior of the longitudinal Brillouin shifts for the  $(\text{AgI})_x(\text{AgPO}_3)_{1-x}$  glasses: (o)  $x = 0.55$ ; ( $\diamond$ )  $x = 0.4$ ; (+)  $x = 0.3$ ; (x)  $x = 0.2$ ; ( $\bullet$ )  $x = 0.1$ ; ( $\square$ )  $x = 0.0$ .

loun doublet as an internal standard. We have therefore measured the room-temperature Brillouin intensities at a given experimental condition (i.e., laser power, slits width, etc.) merely changing the samples. The obtained data are reported in column 6 of Table I, where a linear increase of Brillouin intensities is shown together with the AgI content. An evaluation of the Brillouin intensity<sup>15</sup> using the Lorentz-Lorenz relation<sup>16</sup> to calculate the polarizability cannot account for the measured increase, which is found to be more than 2.5 from  $x = 0.0$  to  $x = 0.55$ .

A better result can be obtained if we consider the polarizability modification due to long-range interaction.<sup>17</sup> From the work of Mazzacurati *et al.*,<sup>17</sup> the measured Brillouin intensities can be written as

$$I \propto \frac{\tau}{\rho v_L^2 n^2} \left[ (n^2 - 1)^2 \left( 1 + \frac{n^2 - 1}{5} \right)^2 \right], \quad (3)$$

where  $\rho$  is the mass density,  $v_L$  is the longitudinal sound velocity,  $n$  is the refractive index, and  $\tau = 2/(n+1)^2 2n/(n+1)^2$  accounts for the transmission at the two vacuum-sample interfaces.

Following Eq. (3), the theoretical behavior of the Brillouin intensity versus AgI concentration has been evaluated (see column 7 of Table I) using the available data for

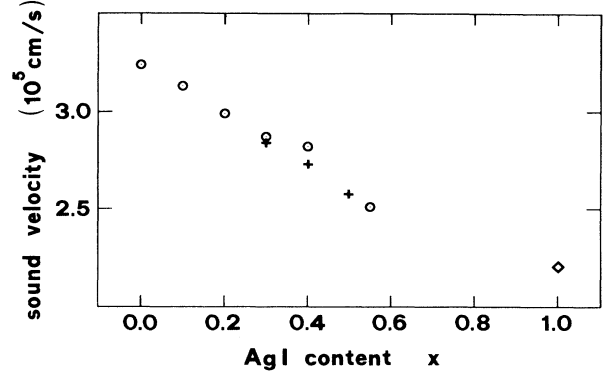


FIG. 6. Room-temperature sound velocities (see Table I) as a function of AgI concentration (circles). Crosses and the  $\alpha$ -AgI longitudinal sound velocity ( $\diamond$ ) are from Ref. 14.

the refractive index (i.e., for  $\lambda=6471 \text{ \AA}$ ). Indeed, as Eq. (3) shows, at high  $n$  ( $n > 2$ ) the predicted Brillouin intensity is strongly  $n$  dependent. The resulting computed data reproduce reasonably the measured trend even if, due to the lack of knowledge of the true refractive index (at  $\lambda = 5145 \text{ \AA}$ ), some differences may be expected. For instance, a variation of 5% in  $n$ —as rough measurements performed by us seem to indicate—is sufficient to reproduce the experimental trend. The agreement between the experimental data and the predicted ones makes us confident in using the Brillouin intensities as a reference for comparing the Raman intensities in different samples.

### 3. High-frequency isotropic spectra

Having verified that the temperature behavior of the isotropic spectrum follows the Bose population factor the trivial temperature dependence of the one-phonon scattering has been taken into account. Hence our intensities evaluations have been done using

$$I_{\text{iso}}^R(\omega) = I_{\text{iso}}(\omega) / [n(\omega, T) + 1] \quad (4)$$

for the Stokes side, where  $I_{\text{iso}}$  is the experimental datum and  $n(\omega, T) = 1/(e^{\hbar\omega/kT} - 1)$ .

The integrated intensity  $I_I$  of the reduced high-frequency contribution to the isotropic spectrum (nor-

TABLE I. Room-temperature measurements of mass density ( $\rho$ ) (present work) and refractive index ( $n$ ) (11) at different AgI concentrations ( $x$ ). From the Brillouin shifts ( $\omega_B$ ) (column 4) the longitudinal sound velocities ( $v_L$ ) are calculated (column 5). In columns 6 and 7 we compare the measured ( $I_B^{\text{expt}}$ ) and the theoretical ( $I_B^{\text{theor}}$ ) trend of the Brillouin intensities versus AgI content (see text). The intensities are normalized to the one at  $x = 0$ .

$x$	$n$	$\rho$ (g/cm)	$\omega_B$ (cm <sup>-1</sup> )	$v_L$ (10 <sup>5</sup> cm/sec)	$I_B^{\text{expt}}$	$I_B^{\text{theor}}$
0.0	1.79	4.45	0.532	3.24	1.0	1.0
0.1	1.83	4.70	0.525	3.13	1.28	1.13
0.2	1.86	4.85	0.509	2.99	1.75	1.30
0.3	1.90	5.02	0.500	2.87	2.04	1.51
0.4	1.93	5.21	0.499	2.82	2.62	1.62
0.55	2.1	5.43	0.484	2.51		2.92

malized to the Brillouin ones) may be therefore evaluated (see Table II, column 2) and we have found that this intensity closely follows the increase of the AgI content. It is well known<sup>18,19</sup> that in the Raman spectrum of  $\alpha$ -AgI a broadband centered around  $110\text{ cm}^{-1}$  is present, the origin of which has been assigned to the optical-phonon density of states. On the other hand, in the Raman spectra of silver-borate glasses the same band appears around  $110\text{ cm}^{-1}$  and increases with the AgI concentration,<sup>8</sup> indicating that the dynamics of these glasses in this frequency region is very similar to that of  $\alpha$ -AgI. The present data regarding the Raman intensity in the phosphate glasses show in a quantitative way that the polarized band at  $110\text{ cm}^{-1}$  can be assigned to the AgI optical density of states.

### B. Anisotropic scattering

With the aim of evaluating the integrated intensity of the one-phonon contribution to the anisotropic scattering, the temperature evolution of the anisotropic spectral shape has been analyzed at each given AgI content (see, for instance, Fig. 2, where the anisotropic spectra of the  $x = 0.55$  glass at several temperatures are shown).

It may be noted that (see Fig. 7), while no difference is observable in the spectral shape of the reduced spectra for  $\omega > 20\text{ cm}^{-1}$ , at low frequencies the QES appears and its intensity is strongly temperature dependent. By means of this different temperature behavior we are able to separate these two contributions, merely subtracting the reduced spectrum at 18 K from the ones at all other temperatures. Using this kind of procedure, a systematic error due to the nonzero quasielastic scattering contribution at low temperature may be introduced. However, an evaluation of this QES contribution to the anisotropic spectra at 18 K shows that it amounts to less than 5% of the total one-phonon scattering.

This procedure has been repeated at all measured concentrations of silver iodide and therefore we have extracted the one-phonon contribution.

In this paper we will focus our attention on a quantitative description of the one-phonon contribution, while a full discussion of the QES contribution (which also needs higher-temperature data) will be presented in a future

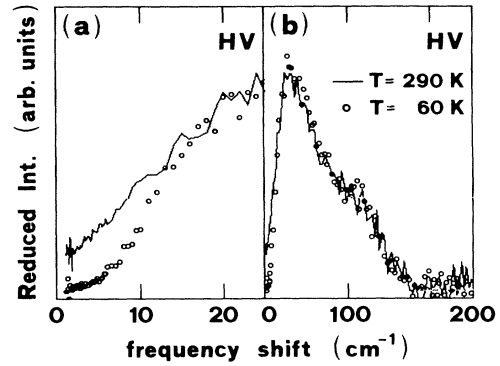


FIG. 7. Reduced intensity  $I(\omega)/[n(\omega, T) + 1]$  at two different temperatures: circles for  $T = 60\text{ K}$ , solid line for  $T = 290\text{ K}$ , both for the  $x = 0.55$  glass. In (a) the QES is evident. Let us note (b) that over  $30\text{ cm}^{-1}$  the spectral shapes are the same.

paper.

Recalling the definitions given in Eqs. (1) and (2), the Brillouin intensity has been used again as a reference to evaluate the intensity of the one-phonon anisotropic scattering at all the AgI concentrations (see Table II, column 3). There, it can be seen that the intensity of the anisotropic spectrum is an increasing function of the AgI content. All the information we have presented up to now could suggest that the whole spectrum can be regarded as a superposition of the spectra of the pure  $\alpha$ -AgI and  $\text{AgPO}_3$  components. In fact, (i) the anisotropic as well as the isotropic one-phonon integrated intensities are monotonic functions of  $x$ ; (ii) the  $\text{PO}_4$  molecular structures at  $675\text{ cm}^{-1}$  just change their intensity as a function of  $x$ , this being due trivially to the increasing AgI content;<sup>12,13</sup> (iii) many authors<sup>4,6-9,12,14</sup> support the hypothesis that two species that are  $\text{AgPO}_3$ -like and  $\alpha$ -AgI-like should coexist in this glassy material even if the dimensions and the spatial distribution of this kind of cluster is still a controversial problem.

Hence we have made the rough hypothesis that the whole one-phonon density of states can be regarded as a superposition of the  $\text{AgPO}_3$  and  $\alpha$ -AgI spectra. In order to check this hypothesis, some test measurements on an  $\alpha$ -AgI single crystal have been performed<sup>20</sup> and a tentative reconstruction of the one-phonon glass spectral shape has been obtained by using

$$I(\omega)_{\text{aniso}}^{\text{glass}} = aI(\omega)_{\text{aniso}}^{\text{AgPO}_3} + bI(\omega)_{\text{aniso}}^{\alpha\text{-AgI}}. \quad (5)$$

We can expect that this kind of reconstruction could work in the frequency range where only the one-phonon scattering contributes to the anisotropic spectrum.

Because glasses and pure  $\alpha$ -AgI do not exist at the same temperature, room-temperature anisotropic spectra of glasses have been obtained using in Eq. (5)

$$I_{\text{aniso}}^{\alpha\text{-AgI}}(\omega, T = 290\text{ K}) = I_{\text{aniso}}^{\alpha\text{-AgI}}(\omega, T = 490\text{ K}) \times \frac{n(\omega, T = 290\text{ K}) + 1}{n(\omega, T = 490\text{ K}) + 1}. \quad (6)$$

TABLE II. Integrated intensities vs AgI content ( $x$ ) of the different contribution to the Raman spectra. Intensities are measured with respect to the Brillouin ones. Column 2 regards the one-phonon contribution to the isotropic spectra ( $I_I$ ) while column 3 regards the anisotropic one ( $I_A$ ).

$x$	$I_I$	$I_A$
0.0	0	$42 \pm 8$
0.1	$15 \pm 3$	$95 \pm 19$
0.2	$22 \pm 4$	$127 \pm 25$
0.3	$36 \pm 7$	$163 \pm 32$
0.4	$35 \pm 7$	$150 \pm 30$
0.55	$53 \pm 10$	$190 \pm 38$

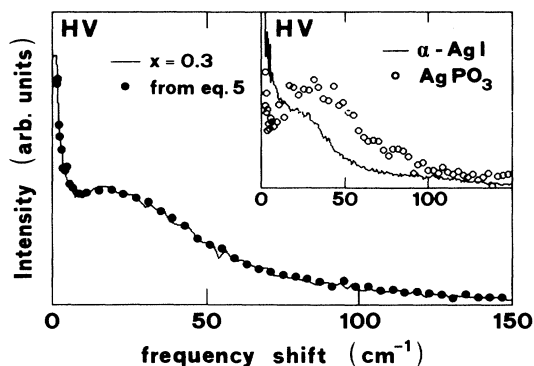


FIG. 8. Reconstruction of the room-temperature  $x = 0.3$  experimental anisotropic spectrum using Eq. (5). Solid line, experimental data; dots, reconstruction. The inset shows the  $\alpha$ -AgI (—) and  $\text{AgPO}_3$  (o) spectra used to obtain the reconstruction.

As an example, in Fig. 8 the whole anisotropic spectrum (i.e., one-phonon + QES contribution) of the  $x = 0.3$  glass is shown together with the one obtained following Eq. (5). The agreement may be considered satisfactory for  $\omega > 10 \text{ cm}^{-1}$  for all  $x$  values, while at lower frequencies, where the QES contribution becomes predominant in the glass spectrum, we found discrepancies that become greater at high  $x$  values. Indeed, while in the frequency range  $5 < \omega < 200 \text{ cm}^{-1}$ , the  $\alpha$ -AgI spectrum is known to be due to the one-phonon density of states,<sup>19</sup> the scattering contributions to the very-low-frequency domain are still an open problem (Ref. 19 and references quoted therein), and therefore we cannot expect that our reconstruction could be extended to this frequency range.

We have also found that the ratio  $b/a$  of the coefficients in Eq. (5) (roughly 30%) behaves as  $x/(1-x)$ . In Fig. 9 we report such values together with the expected curve.

## V. CONCLUSION

Thanks to the possibility of having reliable data of Brillouin and Raman scattering, we have analyzed in a quantitative way the diverse spectral components. The behavior of the isotropic and the anisotropic parts of the spectra as a function of temperature and AgI content suggests the hypothesis that the dynamics of the glass  $(\text{AgI})_x(\text{AgPO}_3)_{1-x}$  can be explained considering the glass as being formed by two weakly interacting phases: the pure  $\alpha$ -AgI-like phase and the  $\text{AgPO}_3$  phase. Indeed, this kind of hypothesis has been done for silver-borate glasses whose dynamics seems to be very close to the silver-phosphate ones (see the discussion of the previous section).

As a matter of fact, extended x-ray-absorption fine structure (EXAFS),<sup>21</sup> neutron diffraction,<sup>22</sup> and Raman-

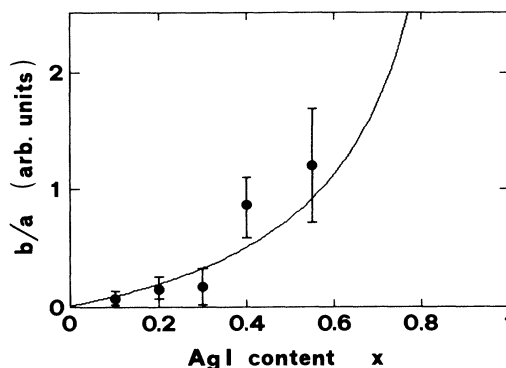


FIG. 9. Ratio of the coefficient ( $b/a$ ) used in the reconstruction of the experimental anisotropic spectra as a function of AgI content. The solid line is the function  $x/(1-x)$ .

scattering<sup>6-8</sup> measurements on silver-borate glasses indicate the presence of "amorphous"  $\alpha$ -AgI-like clusters. The dimension and the spatial distribution of these clusters are still an open problem even if neutron diffraction and Raman measurements indicate that they are about 20–30 Å.

Our data regarding silver-phosphate glasses are compatible with the presence of such clusters even if Brillouin measurements (present work and Ref. 11) indicate that their dimension has to be much smaller than the wavelength of the measured acoustic mode. The behavior of the isotropic as well as the anisotropic spectra is consistent with the presence of two weakly interacting phases. Regardless, there would not be crystalline microdomains within the glass matrix: a partial order due to the presence of fixed iodine in a cubic arrangement, as in  $\alpha$ -AgI is not possible; rather, we would be faced with an "amorphous phase" of silver iodide.

Indication on the dimension of the clusters could be inferred by using the Martin and Brenig model,<sup>23</sup> i. e. from an accurate analysis of the low frequency spectral shape of the vibrational density of states.<sup>6</sup> Our study of the temperature behavior of the spectral shape would enable us to carefully describe this frequency domain, thanks to the possibility of distinguishing the QES from the one-phonon density of states. Works are in progress in this direction.

## ACKNOWLEDGMENTS

We wish to thank Dr. A. Tomasi for having grown and characterized our sample. One of the authors (P.A.M.R.) undertook this work with the support of the International Centre for Theoretical Physics (ICTP) Program for Training and Research in Italian Laboratories, Trieste, Italy.

- \*Permanent address: Departamento de Fisica, Universidade Estadual de Campinas, Campinas, CEP-13081, São Paulo, Brazil.
- <sup>1</sup>T. Minami and M. Tanaka, *Rev. Chim. Min.* **16**, 283 (1979).
- <sup>2</sup>For a review, see *Superionic Conductors*, edited by G. D. Mahan and R. Alben (Plenum, New York, 1976); *Fast Ion Transport in Solids*, edited by P. Vashista and J. N. Mundy (North-Holland, Amsterdam, 1979).
- <sup>3</sup>M. Tachez, R. Mercier, J. P. Malugani, and P. Chieux, *Solid State Ion.* **25**, 263 (1987).
- <sup>4</sup>M. Tachez, R. Mercier, J. P. Malugani, and A. J. Dianoux, *Solid State Ion.* **20**, 93 (1986).
- <sup>5</sup>M. Tachez, J. P. Malugani, R. Mercier, and P. Chieux, *Annu. Report* (1984), Institut Laue-Langevin, Grenoble, France.
- <sup>6</sup>G. Carini, M. Cutroni, A. Fontana, G. Mariotto, and F. Rocca, *Phys. Rev. B* **29**, 3567 (1984).
- <sup>7</sup>A. Fontana, G. Mariotto, and F. Rocca, *Phys. Status Solidi B* **129**, 489 (1985).
- <sup>8</sup>A. Fontana and F. Rocca, *Phys. Rev. B* **36**, 9279 (1987).
- <sup>9</sup>A. Fontana, F. Rocca, and M. P. Fontana, *Phys. Rev. Lett.* **58**, 503 (1987); A. Fontana, F. Rocca, M. P. Fontana, B. Rosi, and A. J. Dianoux, *Phys. Rev. B* **41**, 3778 (1990).
- <sup>10</sup>V. Mazzacurati, P. Benassi, and G. Ruocco, *J. Phys. E* **21**, 798 (1988).
- <sup>11</sup>L. Borjesson, Ph.D. thesis, Chalmers University of Technology of Goteborg, Goteborg, Sweden, 1987.
- <sup>12</sup>J. P. Malugani and R. Mercier, *Solid State Ion.* **13**, 293 (1984).
- <sup>13</sup>A. Fontana, F. Rocca, and A. Tomasi, *J. Non-Cryst. Solids* **123**, 230 (1990).
- <sup>14</sup>L. Borjesson and L. M. Torell, *Phys. Lett.* **107A**, 190 (1985).
- <sup>15</sup>B. J. Berne and R. Pecora, *Dynamics Light Scattering* (Wiley, New York, 1976).
- <sup>16</sup>M. Born and E. Wolf, *Principles of Optics*, 4th ed. (Pergamon, Oxford, 1970), p. 87.
- <sup>17</sup>V. Mazzacurati, M. Nardone, G. Ruocco, and G. Signorelli, *Philos. Mag. B* **59**, 3 (1989).
- <sup>18</sup>G. L. Bottger and L. Geddes, *J. Chem. Phys.* **46**, 3000 (1976); M. J. Delaney and S. Ushioda, *Solid State Commun.* **19**, 297 (1976).
- <sup>19</sup>E. Cazzanelli, A. Fontana, G. Mariotto, V. Mazzacurati, G. Ruocco, and G. Signorelli, *Phys. Rev. B* **28**, 7269 (1983).
- <sup>20</sup>P. Benassi, L. Borjesson, A. Fontana, V. Mazzacurati, G. Signorelli, and G. Ruocco (unpublished results).
- <sup>21</sup>F. Rocca, G. Dalba, and P. Fornasini, *Mater. Chem. Phys.* **23**, 85 (1989).
- <sup>22</sup>L. Borjesson, L. M. Torell, U. Dahlborg, and W. S. Howells, *Phys. Rev. B* **39**, 3404 (1989).
- <sup>23</sup>A. Martin and W. Brenig, *Phys. Status Solidi B* **64**, 163 (1974).